Muffin-tin Green's-function theory of hydrogen defects in aluminum

B. M. Klein and W. E. Pickett
Condensed Matter Physics Branch, Naval Research Laboratory, Washington, D.C. 20375
(Received 31 August 1983)

We present results of a muffin-tin Green's-function-method study of interstitial or substitutional hydrogen impurities in an aluminum host lattice. The calculations are based on an extended-charge single-site approximation discussed previously, whereby the effects due to the H-impurity charge density outside of the impurity muffin tin are included approximately. The host aluminum Green's function is determined from augmented-plane-wave energy-band calculations performed in the local-density approximation for the exchange and correlation. The H-impurity charge and state densities are presented and compared with previous calculations using different methods. Muon Knight shifts, proton spin-lattice relaxation rates, and residual resistivities have been determined and are compared with experiment where available, and with other calculations.

I. INTRODUCTION

There has been considerable interest in studying the effects of hydrogen in metals due in part to the simplicity of a proton impurity in a host metal and, more recently, due to the possible technological importance of metal-hydrogen systems as, for instance, hydrogen storage media and high-temperature superconductors.[1] A large body of literature exists regarding theoretical studies of stoichiometric hydride systems, such as PdH, using standard energy-band techniques,[2] while a variety of different methods have been used to investigate hydrogen impurities in metals in the dilute limit.[3] In this paper we use the recently refined muffin-tin Green's-function (MTGF) method to study the effects of an isolated hydrogen point-charge impurity in the simple *sp* metal aluminum. Calculations using the methods employed here have been reported by the authors for H impurities in Pd (Ref. 4) and in ZrV_2 and $ZrCo_2$ (Ref. 5).

We consider a proton impurity at three different locations in the fcc Al host: (1) an octahedral interstitial site located at $(\frac{1}{2},\frac{1}{2},\frac{1}{2})a$; (2) a tetrahedral interstitial site located at $(\frac{1}{4},\frac{1}{4},\frac{1}{4})a$; (3) a substitutional site where the proton replaces an Al atom. Here a is the cubic lattice constant. From a theoretical point of view, Al is a good system for applying the MTGF method since it is known that hydrogen only weakly dissolves in this metal so that the approximation of neglecting H-H interactions should be good, and in addition, the fact that this system corresponds to a proton embedded in an almost uniform electron gas has made it a good testing ground for more approximate methods with which we can compare our results.

This paper accompanies the preceding paper, hereafter referred to as I,[6] which gives a more extensive discussion of the theoretical and computational techniques that we have used, as well as presenting results for transition-metal impurities and vacancies in Al. The remainder of this paper is organized as follows: Section II gives a brief discussion of some of the relevant MTGF equations used in our calculations; in Sec. III we describe the band-structure techniques used to generate the Al host lattice quantities; in Sec. IV we present and discuss our charge- and state-density and impurity potential results for the H impurities at the three different sites; in Sec. V we compare our results with other theoretical results; in Sec. VI we present calculations of muon Knight shifts, spin-lattice relaxation rates, and residual resistivities and compare these with experiment and other calculations where available; in Sec. VII we present some conclusions.

II. MTGF APPROACH

The theoretical formulation of our version of the MTGF method is fully described in I, so that here we give a brief summary of some of the key equations and their application to the studies of H impurities in Al. The impurity charge density $\rho(r)$ and density of states $N(E)$ can be determined from the Green's function as follows:

$$\rho(r)=-\frac{2}{\pi}\int_{-\infty}^{E_F}\mathrm{Im}G(r,r;E)dE\ , \tag{1}$$

$$N(E)=-\frac{2}{\pi}\int_{0}^{R}\mathrm{Im}G(r,r;E)4\pi r^2 dr\ , \tag{2}$$

with E_F as the Fermi energy (fixed by the host band structure) and R as the particular muffin-tin radius. It has been shown[6,7] that a self-consistent solution for $G(r,r;E)$ in the single-site approximation involves determining a Green's function $\tilde{G}_{LL'}(E)$ in each iteration cycle, where $L=(l,m)$ is an angular momentum index. For impurities at a site of cubic symmetry, $\tilde{G}_{LL'}(E)$ is diagonal in L for $l\leq 2$, and it can be split into $s,p,d(e_g)$ and $d(t_{2g})$ components, each of which can be determined from linear equations involving host band-structure quantities (angular momentum components of the density of states and radial wave functions) and host and impurity potential phase shifts. The substitutional and octahedral H-impurity sites in Al indeed have cubic symmetry, while the tetrahedral-site symmetry is lower than cubic. In the latter calculation we neglected the (in this case) small non-

cubic coupling terms between the p and d channels. For all of the calculations we used an $l_{\max}=3$, once again neglecting small nondiagonal coupling terms between $l=3$ and $l<3$.

The self-consistent iteration scheme is begun by taking an initial guess at the impurity muffin-tin potential, close to the form of a hydrogen-atom potential in the present case, and together with the host quantities described in the next section obtaining a solution for $\tilde{G}_{LL'}(E)$. $G(r,r;E)$ and $\rho(r)$ are then determined so that a new impurity Coulombic and exchange-correlation potential can be constructed and the iteration scheme is continued (see I for more details). Using a simple linear mixing scheme for successive old and new potentials for a subsequent iteration leads to rapid convergence for the problems considered here. Starting with a 90% old, 10% new mixing for approximately five cycles, and subsequently switching to 75/25 mixing leads to convergence of the impurity potential to $\approx 10^{-4}$ Ry rms in 15–20 total cycles.

III. APW CALCULATIONS

The Al-host energy bands were calculated using the self-consistent (SC) augmented-plane-wave (APW) approach[8] with the Hedin-Lundqvist[9] form of the local-density exchange-correlation potential. Scalar relativistic effects (neglecting the spin-orbit interaction) were included following the method of Koelling and Harmon.[10] The Al core electrons [Ne] were treated in the soft-core approximation, with the core charge density being recalculated in each SC cycle using the crystal potential from the previous cycle as input into the fully relativistic atomic-structure code of Liberman *et al.*[11] After beginning the SC iterations on a 6–$\vec{k}$-point mesh in the irreducible Brillouin zone, a series of final iterations on a 20–$\vec{k}$-point mesh were used for the final convergence runs. The Al eigenvalues were highly converged to better than 1 mRy in all cases. The final 20–$\vec{k}$-point mesh eigenvalues were interpolated onto a mesh of 89 $\vec{k}$ points using the symmetrized Fourier method of Boyer,[12] and the densities of states were determined using tetrahedral integration.[13] The procedures used to generate the host lattice quantities are somewhat different from that used in I (Ref. 14) for reasons which follow.

The band structure for the Al host was done for an fcc unit cell with three inequivalent lattice sites: one octahedral site containing an Al nucleus with $Z=13$ hereafter referred to as the Al site, another independent octahedral interstitial site with zero nuclear charge, and a pair of equivalent interstitial sites with tetrahedral symmetry with zero nuclear charge. The octahedral and tetrahedral interstitial "empty-sphere" sites form the muffin-tin hosts for the subsequent interstitial H-impurity calculations, while the Al-atom muffin tin is used as the host for the case of substitutional H.

The crystal structure dictates constraints on the maximum muffin-tin sphere radii so that the spheres do not overlap. Calling the three sphere radii $R_{\rm Al}$, $R_{\rm oct}$, and $R_{\rm tet}$, these constraints are, measured in a.u.,

$$R_{\rm Al}+R_{\rm tet}\le(\sqrt{3}/4)a=3.306\ ,$$

$$R_{\rm tet}+R_{\rm oct}\le(\sqrt{3}/4)a=3.306\ ,$$

$$R_{\rm Al}+R_{\rm oct}\le a/2=3.817\ ,$$

where we have substituted for the Al lattice constant $a=4.04$ Å$=7.635$ a.u. If it were not for the empty spheres at the octahedral (oct) and tetrahedral (tet) sites, maximum Al sphere radii of $(\sqrt{2}/4)a=2.7$ a.u. could be used for the simple fcc structure. However, to ensure meaningful results for the tetrahedral site we chose $R_{\rm tet}=1.0$ a.u. which limited the value of $R_{\rm Al}$. The muffin-tin sphere radii used were, measured in a.u.,

$$R_{\rm Al}=2.306\ ,$$

$$R_{\rm oct}=1.490\ ,$$

$$R_{\rm tet}=1.000\ .$$

The resulting band structure for Al was very similar to that obtained by others (e.g., see Moruzzi *et al.*[15] who used the SC Korringer-Kohn-Rostoker method with Hedin-Lundqvist exchange correlation). The width of the occupied valence bands was 0.814 Ry, and the energy bands and densities of states were calculated up to more than 1.5 Ry above the Fermi energy E_F in order to do the Kramers-Kronig transforms for the real part of the host Green's functions.[6,7]

IV. CHARGE AND STATE DENSITIES

In Figs. 1–4 we show the electronic charge and state densities for H impurities in the octahedral and tetrahedral interstices and in the substitutional position. The charge and state densities have been determined from the impurity Green's functions using Eqs. (1) and (2), respectively. In Fig. 1 we show for comparison the charge density for an unperturbed hydrogen atom embedded at the impurity site added to the charge density of the unperturbed host. For the substitutional case the atomic hydrogen charge density was added to that of the Al vacancy as calculated in paper I. Table I contains additional information relevant to our discussion of the charge and state densities.

From Fig. 1 we see that the *interstitial* proton attracts more electronic charge close to the site compared with the H atom, especially for the tetrahedral case, so that the proton impurity is more effectively screened compared to the free atom. As would be expected from the charge-density results, the tetrahedral-site potential should be the most attractive, followed by the octahedral and substitutional sites, respectively. This is borne out by our numerical results. In fact, the attractive tetrahedral-site potential is sufficiently strong so that an s-like bound state is formed (see Table I). A bound state does not form at the octahedral site, although it almost does, with a sharp s resonance occurring just above the bottom of the valence bands, as can be seen in Fig. 2. There is no indication of a bound state or resonance for the substitutional case. The s bound state for the tetrahedral H impurity contains 0.333 electrons in the muffin tin, slightly less than half of the total impurity s-like muffin-tin charge Q_s. Since the bound state can hold a total of two electrons, this shows

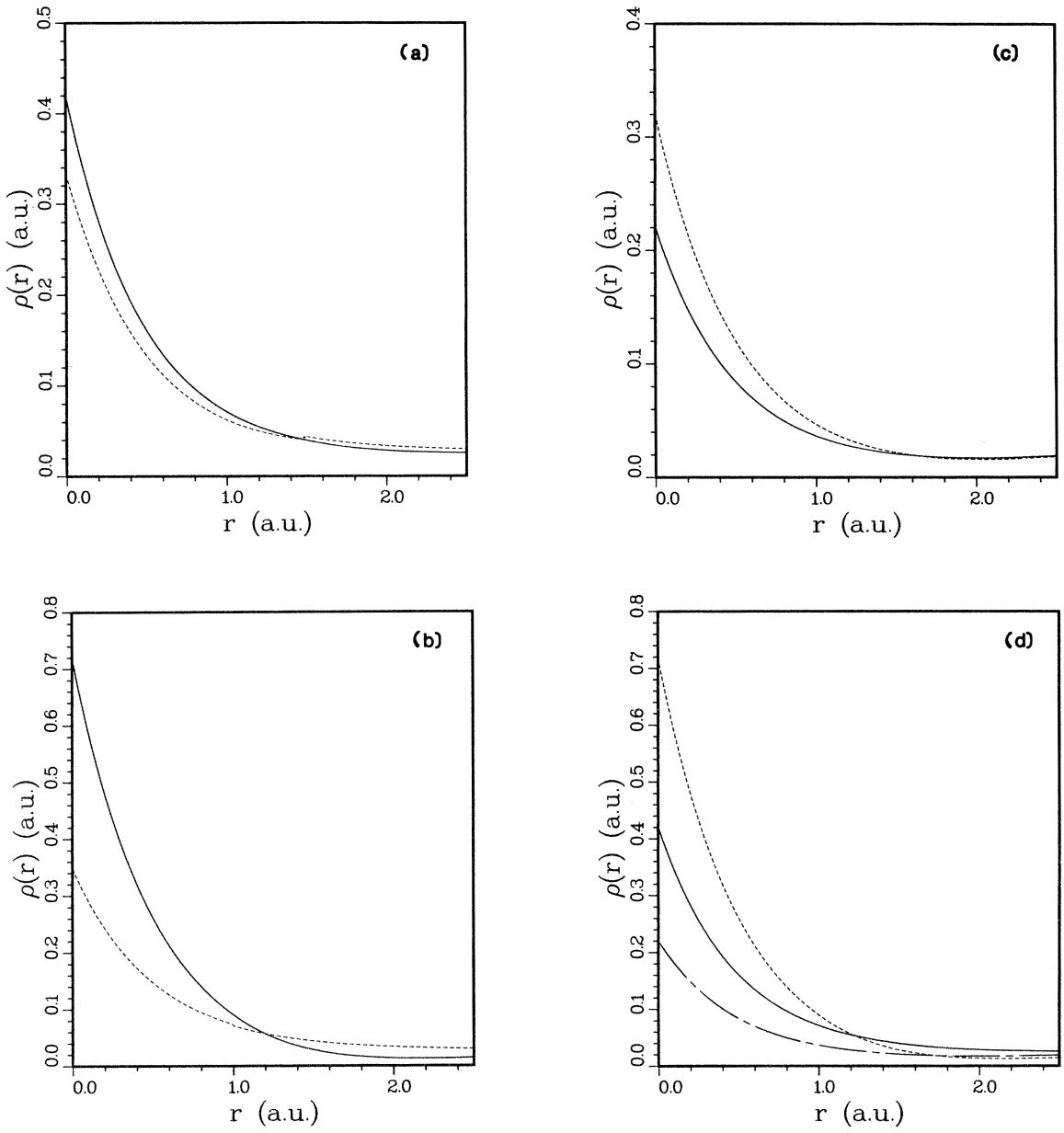

FIG. 1. SC MTGF H-impurity electronic charge densities (solid curves) and free H-atom electronic charge densities plus the host background densities (dashed curves) in Al for (a) octahedral interstitial location; (b) tetrahedral interstitial location; (c) substitutional location; (d) shows the three MTGF results on the same scale: (——) octahedral, (— — —) tetrahedral, and (—·—) substitutional.

TABLE I. H-impurity MT radii R_{MT}; H-impurity electronic charges Q_s, Q_p, $Q_{tot}=Q_s+Q_p+Q_d+Q_f$, and Q_s^{bs} (bound state, included in Q_s); ΔZ_{Lloyd} and $\Delta Q=Q_{tot}-Q_{host}$; H-impurity charge density at the origin, $\rho(0)$; bound-state energy relative to the bottom of the valence band, E_{bs}.

	R_{MT} (a.u.)	Q_s (e)	Q_s^{bs} (e)	Q_p (e)	Q_{tot} (e)	ΔZ_{Lloyd} (e)	ΔQ (e)	$\rho(0)$ (a.u.)	E_{bs} (eV)
H_{oct} in Al	1.49	0.834	0.0	0.124	0.963	0.910	0.681	0.420	
H_{tet} in Al	1.0	0.692	0.333	0.017	0.708	0.630	0.584	0.719	−0.381
H_{sub} in Al	2.306	0.777	0.0	0.267	1.097	−0.886	−0.332	0.203	

that the bound-state wave function is quite extended in the crystal, and is an indication of the sensitivity of its location (in energy) relative to the host bands. It should come as no surprise, therefore, that the bound-state position is sensitive to the inclusion of the charge-density tail correction discussed in paper I. We find that neglecting this tail correction causes a downward shift in the bound-state energy of several tenths of an eV for the tetrahedral case, and the appearance of a bound state at the octahedral site just at the bottom of the octahedral site valence bands.

We now turn to the density-of-states (DOS) results shown in Figs. 2–4. The H-impurity DOS for the interstitial cases shows a strong enhancement of $N_s(E)$ near the bottom of the host bands, while the $N_p(E)$ results more nearly track the host values with a fairly uniform enhancement. The s bound state for the tetrahedral site and the strong s resonance for the octahedral case should be noted in Figs. 2 and 3, respectively. It is also worth noting that the peaks in the impurity DOS do not always line up with peaks in the host DOS, even at higher energies, as can be seen by examining Figs. 2 and 3 at approximately -2 eV. The results for substitutional H shown in Fig. 4 are qualitatively different from the interstitial cases, with the notable absence of enhancement of $N_s(E)$ near the bottom of the Al bands, and the diminution of $N_p(E)$ and $N_d(E)$ (not shown) compared to the host. The proton is not nearly as effective in pulling in screening electrons for the substitutional case, as noted above in our discussion of the charge density.

In Table I we also show results for the local impurity charges Q_l, $Q_{\text{tot}}=\sum_{l=0}^{3}Q_l$, ΔQ defined as $Q_{\text{tot}}-Q_{\text{host}}$,

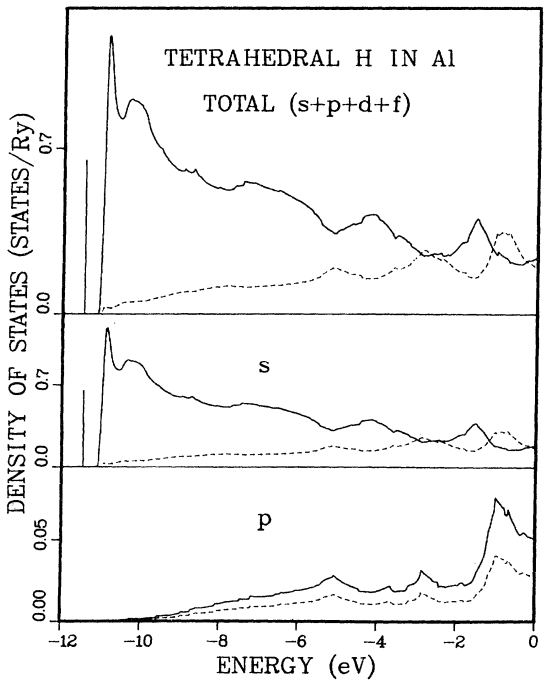

FIG. 3. SC MTGF H-impurity local DOS's (solid curves) and host local DOS's (dashed curves) for the tetrahedral interstitial site in Al. The s bound state is shown as a vertical line in the upper two panels below the band bottom. The Fermi level is at $E=0.0$.

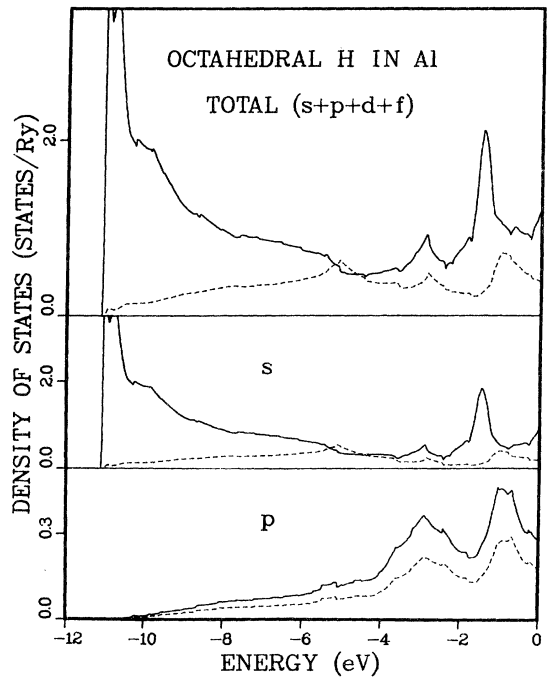

FIG. 2. SC MTGF H-impurity local DOS's (solid curves) and host local DOS's (dashed curves) for an octahedral interstitial site in Al. The Fermi level is at $E=0.0$.

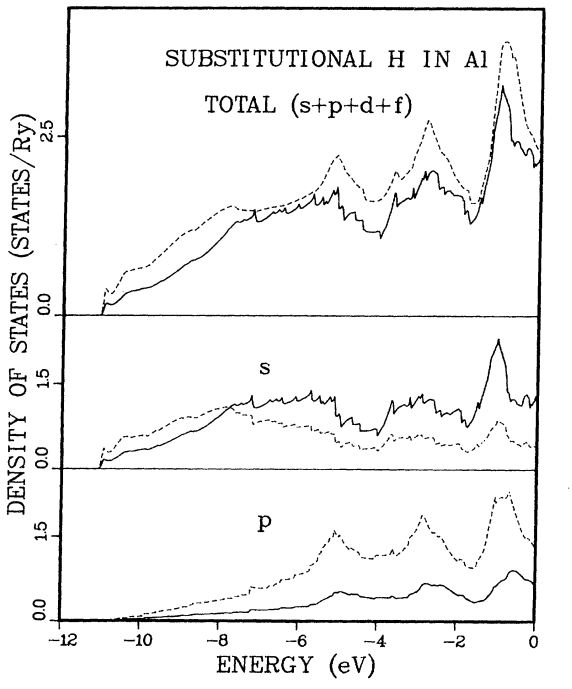

FIG. 4. SC MTGF H-impurity local DOS's (solid curves) and host local DOS's (dashed curves) for a substitutional site in Al. The Fermi level is at $E=0.0$.

and ΔZ which has been determined from the Lloyd formula in the single-site approximation as given in I. It can be argued that the difference between ΔZ and ΔQ gives an indication of the relative importance of considering the effects of electronic charge relaxation beyond the impurity muffin tin, which is partially compensated by our inclusion of the impurity charge density outside the defect muffin tin. It can be seen from Table I that ΔZ and ΔQ are in agreement on a scale of 25% for the interstitial cases, while ΔQ is less than half the value of ΔZ for the case of substitutional H. This is what one might expect since the single-site approximation is the most suspect in the latter case. That is, substituting a proton ($Z=1$) for an aluminum nucleus ($Z=13$) may lead to a bigger perturbation on the surrounding aluminum atoms than an interstitial proton.

V. COMPARISON WITH PREVIOUS CALCULATIONS

Previous theoretical studies of H (or equivalently, fixed-muon) impurities in Al have made use of five different generic approaches: (1) jellium models[16–26] where the impurity is embedded in an Al host which is approximated by a homogeneous interacting electron gas neutralized by a rigid, uniform positive background charge representing the (smeared-out) ionic cores; (2) pseudopotential models, such as the spherical solid model (SSM) of Ambladh and von Barth[27] and Ambladh *et al.*[28] used by Manninen and Nieminen,[29] Khan *et al.*, and Perrot *et al.*,[30–33] whereby the structureless Al host charge density assumed in the jellium model is improved upon by the introduction of a spherically averaged empirical pseudopotential; (3) molecular-cluster methods[34,35] which consider the H impurity together with a number of Al neighbors forming a finite molecularlike system; (4) Green's-function methods[36–38] such as that used in the present work which attempt to describe the impurity-system Green's function in terms of that of the host lattice which reproduces the electronic structure of bulk Al; (5) supercell methods whereby a large unit cell of impurity and host atoms is periodically repeated so that the impurity problem is solved using conventional band-structure techniques.[39]

There have also been APW band-structure calculations for stoichiometric AlH and AlH_2 (rocksalt and fluorite structures, respectively) with which we can compare our H-impurity results.[40] These calculations were performed assuming an $\sim 5.3\%$ and $\sim 8\%$ lattice constant expansion for the monohydride and dihydride, respectively, and they were non-self-consistent and used an $\alpha=1$ exchange-correlation potential. A striking feature of the AlH results is a low-energy splitoff bonding band involving H-*s* and Al-*s* electrons. This band is found to be 6.44 eV wide and is separated by a gap of 1.17 eV from the next band complex which is an admixture of Al-*sp*—type and H-*sp*—type electrons. The overall energy bands and DOS of AlH bear very little resemblance to metallic Al which shows a nearly parabolic (free-electron-like) behavior. This is in distinction to stoichiometric PdH (Ref. 41) where it has been found that aside from the occurrence of a low-lying H-*s*—Pd-*sd* bonding band, the occupied DOS of PdH is similar in appearance to metallic Pd with the Fermi energy shifted up in energy by somewhat less than one electron. It appears that stoichiometric hydrides of simple *sp* metals such as Al are much more severe modifications of the host band structure than is the case of *d*-band metals such as Pd. It is therefore not surprising that our DOS results for an isolated octahedral H impurity in Al bear only a qualitative resemblance to the H MT DOS in AlH. We do indeed find a pileup of H charge near the bottom of the bands of Al (see Fig. 2), but we do not find a splitoff bound state which we can associate with the results for AlH. The AlH DOS also shows a peak at 2 eV below E_F similar to the peak at $E_F-1.5$ eV shown in Fig. 2.

The band-structure results for AlH_2 are an even more drastic modification of the metallic Al results. For instance, Gupta found[40] that the two lowest-lying bands could be characterized as mainly metal-hydrogen bonding states and hydrogen-hydrogen antibonding combinations. The fact that hydrogen-hydrogen interactions are so important in the dihydride makes a comparison with the case of an isolated tetrahedral H impurity even more tenuous. Although there is some similarity in the H DOS in the two calculations, notably a buildup of states toward the bottom of the bands (see Fig. 3), our calculated tetrahedral-site bound state, which might be indicative of a splitoff band in the dihydride, is not replicated in the stoichiometric calculation.

From the above discussion, it is clear that calculations of an H impurity in Al which take into account charge relaxation beyond the H MT would be particularly useful in generating a more meaningful comparison between the impurity and stoichiometric calculations for Al. We are in the process of generating the capability of performing such calculations. It is to be noted that calculations on H impurities in Pd performed by the authors[4] using the same methods employed here show that the DOS of an octahedral H impurity in Pd is very similar to the corresponding stoichiometric rocksalt-structure hydride results.[41]

There have been numerous papers applying the jellium model[16–26] to study protons and muons in Al with good bibliographies available in Refs. 3 and 26. Very recently, Estreicher and Meier[26] have done a series of calculations of energy profiles of light impurities in metals, including Al, which use the impurity charge densities, $\rho(r)$, calculated within a jellium model, together with a perturbation-theory expression for the site energies involving $\rho(r)$ and a host pseudopotential. Besides giving a number of useful parametrized forms for the jellium results, they also show that the energy profiles are generally extremely sensitive to the choice of empirical pseudopotential. The jellium $\rho(r)$ results for an interstitial proton are, of course, the same for any location, since the only parameter is r_s defined by

$$\bar{\rho}=(4\pi r_s^3/3)^{-1} ,$$

where $\bar{\rho}$ is the average electron density. For Al, $r_s=2.07$, and the jellium calculations show a bound state just below the zero of energy. Although the $\rho(r)$ results are qualitatively similar to those presented here, there are substantial

quantitative differences. For instance, $\rho_{\text{jellium}}(0)=0.50$ a.u. compared with the present values of 0.42 and 0.72 a.u. for octahedral and tetrahedral H, respectively. In the case of substitutional H in Al, an ingenious method has been used to do this calculation within the jellium model, viz., the proton is placed inside a spherical hole set into the jellium system. The underscreening we have found for the substitutional case is also found in the jellium calculations.

Khan *et al.*[30] present SSM results for $\rho(r)$ for H impurities at the same three sites we have considered, and there is good qualitative agreement between their results and ours. The major quantitative difference is that our values of $\rho(r)$ are somewhat higher (lower) than theirs near the proton site for the interstitial (substitutional) cases. Manninen and Nieminen[29] have also done SSM calculations for H in Al but they do not present $\rho(r)$ results with which we can compare (but see the Knight-shift discussion below). The major difference in these two sets of SSM calculations is the choice of pseudopotentials that were used. These choices result in substantial quantitative differences in the calculated heats of solution, and possibly the $\rho(r)$ as well. Both SSM calculations find a bound state only for the tetrahedral case, in agreement with our results.

Recently, Iyakutti *et al.*[35] have performed self-consistent cluster calculations for an Al vacancy and a substitutional proton. Their cluster consists of a central atom (Al or an impurity) and the first shell of 12 neighbors, 13 atoms in all. Comparing our substitutional H with their results, we find agreement in $\rho(r)$ to approximately 5—10%. Although their calculations include electronic charge relaxation at the central site and the first-neighbor shell, their 13-atom cluster is rather small so that we consider the agreement between the two calculations to be satisfactory.

Yussouff and Zeller[36] (YZ) have performed MTGF calculations for H impurities at the octahedral sites in five fcc metals, including Al. Aside from small differences in the Al-host energy-band structure which should be unimportant, the main difference between our calculations and theirs is our inclusion of the impurity charge-density tail correction. YZ obtained a bound state for octahedral H at 2.72 eV below the valence-band bottom while our calculations show instead a strong resonance at the band bottom. This emphasizes the importance of including the charge-density tail correction in the single-site approximation. Further discussion of this point may be found in the recent paper of Braspenning *et al.*[42] where calculations for impurities in Cu (including substitutional H) are discussed in light of their extensions of the MTGF method beyond the single-site approximation. In the paper of YZ,[36] charge- and state-density results are not presented so that further comparisons with their work are not possible.

Craig and Smith[37] and Craig[38] have performed a Green's-function calculation for octahedral or tetrahedral protons in Al. A set of localized real-space functions centered at the impurity site were used to evaluate the host Green's function, and nonspherical corrections to $\rho(\vec{r})$ were included. Craig[38] obtained bound states at 0.001 and 0.43 eV below the band bottom for the octahedral and tetrahedral protons, respectively, in good agreement with our results. There is some disagreement between our $\rho(\vec{r})$ results and his, especially at small r. There is some indication that Craig's calculations have some loss of accuracy, at small r in particular, since his calculations[37] using the same basis function set for jellium disagree with the exact jellium solutions found by other methods. Craig also argues that nonspherical components of $\rho(\vec{r})$ are important in understanding the bonding of H impurities,[38] a conjecture that is in disagreement with the results of other workers[30–33] who found that the contribution of nonspherical terms to the heat of solution of H in Al were $\approx 2-3\%$.

Recently, Gupta[39] performed supercell calculations to study the effects of an octahedral H impurity in Al. His non-self-consistent calculations were based on a supercell containing a total of 27 fcc Al atoms with and without an H impurity present. Gupta found[39] a narrow splitoff Al—H bonding band formed just below ($\sim 0.5-1.0$ eV) the pure Al supercell bands. These results are consistent with what would appear as a bound state just below the Al bands in a MTGF calculation. We expect that Gupta's splitoff band would become even more narrow if the size of his supercell was increased. This is in good qualitative agreement with our finding of a pileup of states near the bottom of the Al bands. Although he does not present DOS results, Gupta does present charge-density results for the H impurity. It is encouraging that his plots of $\rho(r)$ for the H impurity are very similar to our results in Fig. 1(a). He, too, finds that the H impurity appears electronegative compared with the H atom. For example, Gupta's[39] value of $\rho(0)$ is 0.39 a.u. compared with our value of 0.42. The lack of self-consistency in his calculation, which could shift H related states with respect to host states, prevents a more definitive comparison of the two methods for studying defects.

VI. RESULTS FOR OTHER CALCULATED QUANTITIES

A. Muon Knight shift

Muon spin rotation (μSR) experiments are a relatively new technique for probing the effects of hydrogen in metals. The positive muon μ^+ carries one unit of positive charge, similar to a proton, but has $\frac{1}{9}$ the proton mass. Since the μ^+ has some 200 times the mass of an electron, to a first approximation it can be regarded similar to a static point charge, although zero-point motion effects will be considerably larger than for a proton. Proton NMR experiments are more difficult to perform in systems such as Al where the achieved proton concentrations are very small. An excellent review of μSR theory and experiment has been published by Schenck.[43]

In a μSR experiment a polarized μ^+ beam impinges on a sample in an applied magnetic field, B_{ext}. The Larmor precession frequency yields a measure of the induced hyperfine field (hf) at the μ^+ site, B_{hf}, and the Knight shift is defined as

$$K=\frac{dB_{\text{hf}}(0)}{dB_{\text{ext}}}\ , \tag{3}$$

where the muon impurity is taken to be at the origin. The contact hyperfine field at the muon can be written as

$$B_{\rm hf}(0)=(8\pi/3)\mu_B[\rho^+(0)-\rho^-(0)] \quad (4)$$

in terms of $\rho^{\pm}(0)$, the induced spin-up and spin-down densities at the muon site. To evaluate Eq. (4) exactly, the host band structure would need to be determined in a magnetic field $B_{\rm ext}$ yielding a spin-up and spin-down host Green's function which would be used in the MTGF formalism to determine the values of $\rho^{\pm}(0)$ at the muon site. Since we have not done this, we resort to the often used approximation of replacing Eq. (4) by the expression

$$B_{\rm hf}(0)\approx(8\pi/3)\eta_F\chi_s B_{\rm ext} , \quad (5)$$

and

$$K\approx(8\pi/3)\eta_F(0)\chi_s \quad (6)$$

with

$$\eta_F(0)\equiv\Omega\langle\,|\Psi(0)|^2\rangle_{E_F} . \quad (7)$$

Here $\langle\,|\Psi(0)|^2\rangle_{E_F}$ is the wave-function density (normalized in the volume Ω taken as the MT sphere) evaluated at E_F and at the muon site. χ_s is the electronic spin susceptibility of bulk aluminum which we take from experiment.[44]

There are two approximations inherent in Eqs. (6) and (7): The magnetic field dependence of the wave function is neglected, and the induced impurity spin densities are assumed to respond in proportion to the bulk electronic susceptibility. With regard to the former approximation, calculations for jelliumlike models and the spherical solid model[29] show that the true spin-enhancement factor $\rho_s(0)$ which would enter Eqs. (3) and (4) in place of $\eta_F(0)$ is smaller (larger) than $\eta_F(0)$ for the interstitial (substitutional) cases by factors which depend on the r_s values. In Table II we present Knight-shift results for the various cases we have studied. The measured Knight shift is from a room-temperature measurement by Schenck[43] and the experimental value of χ_s we have used is 1.77×10^{-6} emu/cm^3 from Ref. 44.

The different theoretical Knight-shift results show extremely large values for the substitutional case—values more than a factor of 2 larger than the experimental result. It seems safe to conclude that muons are not trapped at vacancy sites in Al. The present results for $\eta_F(0)$ for the interstitial sites are in reasonably good agreement with the results for the spherical solid model.[29] Note that the structureless pure jellium calculations do not distinguish between the different interstitial sites. Our MTGF results for $\eta_F(0)$ for the substitutional muon do differ considerably from the spherical solid model results,[29] but it is to be noted that the latter calculation is more model dependent for the substitutional case.

All of the theoretical results should be corrected for diamagnetic shielding which would lower $K_{\rm theor}$ somewhat.[43] Estimates of this correction by Zaremba and Zobin[45] using a jellium model yield a value of approximately -15 ppm for Al. Including this correction would appear to give a theoretical preference for an octahedral-site occupation for the μ^+ in Al. Recent muon diffusion and trapping studies[46] seem to indicate a preference for octahedral-site occupation at 1 K, however, at higher temperatures mixed octahedral-tetrahedral occupation appears to be observed.[46–48] Unambiguous interpretations of the experiments are difficult because of the effects of other dilute impurities in the Al lattice.[46] Since the Knight-shift measurement[43] is at room temperature, we can conclude that theory and experiment are at least qualitatively consistent.

B. Proton spin-lattice relaxation rate

Although the proton spin-lattice relaxation rate for H in Al has not been measured, we present our theoretical predictions for this quantity defined as[49,50]

$$1/T_1T=4\pi\hbar[N_s(E_F)H_s]^2 , \quad (8)$$

with

$$N_s(E_F)H_s=(8\pi/3)\mu_B[N_s(E_F)\phi_s^2(0,E_F)] , \quad (9)$$

with N_s and ϕ_s as the s density of states and the s radial wave function, respectively, normalized within the MT sphere. Results are presented in Table III. Measurements for H in Al would be very desirable since the theoretical values for T_1T for the octahedral and tetrahedral sites differ by more than a factor of 7. We note that our theoretical MTGF results[51] for H in Pd are in very good agreement with proton NMR experiments.[52]

TABLE II. Theoretical and experimental muon Knight-shift parameters for Al. The notation oct, tet, sub, and interst refer to octahedral, tetrahedral, substitutional, and interstitial (either octahedral or tetrahedral) muon sites, respectively. The Knight shift K has been calculated using $\rho_s(0)$ where available. The experimental value of susceptibility used is 1.77×10^{-6} emu/cm^3 from Ref. 44.

	Present			Spherical solid[a] model			Jellium[a] model		Expt.
	oct	tet	sub	oct	tet	sub	interst	sub	
$\eta_F(0)$	6.88	3.94	12.1	6.92	4.52	19.7	7.76	13.7	
$\rho_s(0)$				6.32	3.36	32.4	7.21	17.2	
K (ppm)	102.0	58.4	179.4	93.4	49.8	480.4	106.9	255.0	79.6(4.0)[b]

[a] Reference 29.
[b] Reference 43.

TABLE III. Theoretical results for the proton spin-lattice relaxation time for octahedral, tetrahedral, and substitutional H in Al.

	$N_s H_s$ (10^{15} G/erg)	$T_1 T$ (sec J)
oct H	7.28	14.41
tet H	2.73	102.5
sub H	6.33	19.06

C. Residual resistivity

An approximate expression for the residual resistivity, ρ_0, for an impurity concentration c is given by,[53] in units of $\mu\Omega$ cm/at. %,

$$\frac{\rho_0}{c} = \frac{2.735\,73}{\sqrt{E_F}} \sum_l (l+1)\sin^2(\eta_{l+1}-\eta_l)\,, \tag{10}$$

where the η_l are the generalized phase shifts defined in I and E_F is to be expressed in Ry. The results are $\rho_0/c = 2.29$, 1.83, and 1.61 $\mu\Omega$ cm/at. % for the octahedral, tetrahedral, and substitutional H impurities, respectively. We are not aware of any experimental measurements of this quantity.

VII. CONCLUSIONS

In this paper we have used the MTGF method to study the effects of isolated hydrogen (or, positive muon) impurities in the simple *sp* metal Al. The resulting charge and state densities have been used to calculate muon Knight shifts, T_1T, and residual resistivities. Comparison of the theoretical and experimental Knight-shift values essentially eliminates the likelihood of substitutional muon occupation; but a more definitive test of the theory, viz., verifying the different results for octahedral- or tetrahedral-site occupation is difficult due to the mixed octahedral-tetrahedral occupations that are observed. Experiments to determine T_1T and the residual resistivity of H in Al would be desirable for making further comparisons.

We have also compared our results with those of previous methods which make use of a variety of techniques. Although we find good quantitative agreement in many cases, nontrivial discrepancies often exist between our results and others. The present MTGF results have the advantage of following from a theory which makes use of an "exact" single-particle host band-structure representation. We have also compared our results with calculations for stoichiometric AlH and AlH_2, and we have found that the H density of states for the isolated impurity has only a qualitative resemblance to the equivalent results for the ordered compounds. It appears, therefore, that H-H interactions are particularly important in the stoichiometric crystals, more so than we have found in similar comparisons in the palladium hydrogen system. This may be a fundamental difference between *sp* and *spd* hydride systems.

Extensions of the MTGF method to go beyond the single-site approximation so as to consider electronic charge relaxation of the host are presently being developed. It will also be important to use the present theory to calculate total electronic energy changes due to impurities, and to include effects due to lattice strains around the defect. Problems such as impurity diffusion will then be amenable to direct first-principles calculation.

ACKNOWLEDGMENT

Discussions of the MTGF method with P. Dederichs and R. Zeller are gratefully acknowledged.

[1]See, e.g., *Hydrogen in Metals I, Basic Properties,* Vol. 28 of *Topics in Applied Physics,* edited by G. Alefeld and J. Volkl (Springer, Berlin, 1978); *Hydrogen in Metals II, Application-Oriented Properties,* Vol. 29 of *Topics in Applied Physics,* edited by G. Alefeld and J. Volkl (Springer, Berlin, 1978).

[2]A. C. Switendick, in *Hydrogen in Metals I, Basic Properties,* Ref. 1, Vol. 28, p. 101; D. A. Papaconstantopoulos, in *Metal Hydrides,* NATO Adv. Studies Inst. Ser., Ser. B, edited by G. Bambikidis (Plenum, New York, 1981), Vol. 76, p. 215.

[3]P. Jena, in *Treatise on Materials Science and Technology,* edited by F. Y. Fradin (Academic, New York, 1981), Vol. 21, p. 351.

[4]B. M. Klein and W. E. Pickett, in *Electronic Structure and Properties of Hydrogen in Metals,* edited by P. Jena and C. B. Satterthwaite (Plenum, New York, 1982), p. 277.

[5]B. M. Klein and W. E. Pickett, J. Less-Common Met. 88, 231 (1982).

[6]W. E. Pickett and B. M. Klein, preceding paper, Phys. Rev. 29, 1588 (1984). A number of references to the MTGF formalism are included in this paper.

[7]R. Zeller and P. H. Dederichs, Phys. Rev. Lett. 42, 1713 (1979); R. Podloucky, R. Zeller, and P. H. Dederichs, Phys. Rev. B 22, 5777 (1980).

[8]See, e.g., L. F. Mattheiss, J. H. Wood, and A. C. Switendick, in *Methods in Computational Physics,* edited by B. Alder, S. Fernbach, and M. Rotenberg (Academic, New York, 1968), Vol. 8.

[9]L. Hedin and B. I. Lundqvist, J. Phys. C 4, 2064 (1971).

[10]D. D. Koelling and B. N. Harmon, J. Phys. C 10, 3107 (1977).

[11]D. A. Liberman, D. T. Cromer, and J. T. Waber, Comput. Phys. Commun. 2, 107 (1971).

[12]L. L. Boyer, Phys. Rev. B 19, 2824 (1979).

[13]G. Lehmann, P. Rennert, M. Taut, and H. Wonn, Phys. Status Solidi 37, K27 (1970); G. Lehmann and M. Taut, *ibid.* 54, 469 (1972); O. Jepsen and O. K. Andersen, Solid State Commun. 9, 1763 (1971).

[14]The major difference is that the occupied portion of the DOS used in Ref. 6 was constructed from APW eigenvalues on a mesh of 240 $\vec{k}$ points in the irreducible wedge of the first Brillouin zone using the results from D. A. Papaconstantopoulos, L. L. Boyer, B. M. Klein, A. R. Williams, V. L. Moruzzi, and J. F. Janak, Phys. Rev. B 15, 4221 (1977).
As mentioned in the text, the host DOS's used here were constructed from APW eigenvalues on a 20—$\vec{k}$-point mesh interpolated onto an 89—$\vec{k}$-point mesh using the method of Ref.

12. Although the DOS used here is somewhat more "noisy" than that of Ref. 6, we believe that this has a relatively minor effect on the present impurity calculations. We emphasize that the reason for recalculating the Al band structure was the need to have the DOS's and potentials for the host interstitial empty MT's.

[15]V. L. Moruzzi, J. F. Janak, and A. R. Williams, *Calculated Electronic Properties of Metals* (Pergamon, New York, 1978).

[16]Z. D. Popovic and M. J. Stott, Phys. Rev. Lett. 33, 1164 (1974).

[17]M. Manninen, R. M. Nieminen, P. Hautojarvi, and J. Arponen, Phys. Rev. B 12, 4012 (1975).

[18]Z. D. Popovic, M. J. Stott, J. P. Carbotte, and G. R. Piercy, Phys. Rev. B 13, 590 (1976).

[19]M. Manninen, J. Phys. F 7, 375 (1977).

[20]A. K. Gupta, P. Jena, and K. S. Singwi, Phys. Rev. B 18, 2712 (1978).

[21]J. K. Norskov, Phys. Rev. B 20, 446 (1978).

[22]D. S. Larsen and J. K. Norskov, J. Phys. F 9, 1975 (1979).

[23]P. Jena and K. S. Singwi, Phys. Rev. B 17, 3518 (1978).

[24]M. I. Darby, M. N. Reed, and K. N. R. Taylor, Phys. Status Solidi A 50, 203 (1978).

[25]P. Jena, Hyperfine Interact. 6, 5 (1979).

[26]S. Estreicher and P. F. Meier, Phys. Rev. B 27, 642 (1983).

[27]C. O. Ambladh and U. von Barth, Phys. Rev. B 13, 3307 (1976).

[28]C. O. Ambladh, U. von Barth, Z. D. Popovic, and M. J. Stott, Phys. Rev. B 14, 2250 (1976).

[29]M. Manninen and R. M. Nieminen, J. Phys. F 9, 1333 (1979).

[30]L. M. Khan, F. Perrot, and M. Rasolt, Phys. Rev. B 21, 5594 (1980).

[31]F. Perrot and M. Rasolt, Solid State Commun. 36, 579 (1980).

[32]F. Perrot and M. Rasolt, Phys. Rev. B 23, 6534 (1981).

[33]F. Perrot and M. Rasolt, Phys. Rev. B 27, 3273 (1983).

[34]P. Jena, F. Y. Fradin, and D. E. Ellis, Phys. Rev. B 20, 3543 (1979).

[35]K. Iyakutti, J.-L. Calais, and A. H. Tang Kai, J. Phys. F 13, 1 (1983).

[36]M. Yussouff and R. Zeller, in *Recent Developments in Condensed Matter Physics,* edited by J. T. Devreese, L. F. Lemmens, V. E. Van Doren (Plenum, New York, 1981), Vol. 3, p. 135.

[37]B. I. Craig and P. V. Smith, Phys. Status Solidi B 113, 747 (1982).

[38]B. I. Craig, Phys. Status Solidi B 114, 337 (1982).

[39]R. P. Gupta, J. Less-Common Met. 88, 299 (1982); in *Electronic Structure and Properties of Hydrogen in Metals,* Ref. 4, p. 283.

[40]M. Gupta, J. Phys. (Paris) 41, 1009 (1980).

[41]See, e.g., D. A. Papaconstantopoulos, B. M. Klein, E. N. Economou, and L. L. Boyer, Phys. Rev. B 17, 141 (1978), as well as Ref. 2 and references therein.

[42]P. J. Braspenning, R. Zeller, A. Lodder, and P. H. Dederichs, Phys. Rev. B (in press).

[43]A. Schenck, Helv. Phys. Acta 54, 471 (1981).

[44]G. L. Dunifer, M. R. Pattison, and T. M. Hsu, Phys. Rev. B 15, 315 (1977).

[45]E. Zaremba and D. Zobin, Phys. Rev. B 22, 5490 (1980).

[46]K. W. Kehr, D. Richter, J.-M. Welter, O. Hartmann, E. Karlsson, L. O. Norlin, T. O. Niinikoski, and A. Yaoans, Phys. Rev. B 26, 567 (1982).

[47]J. P. Bugeat, A. C. Chami, and E. Ligeon, Phys. Lett. 58A, 127 (1976); J. P. Bugeat and E. Ligeon, *ibid.* 71A, 1055 (1979).

[48]O. Hartmann, E. Karlsson, L. O. Norlin, D. Richter, and T. O. Niinikoski, Phys. Rev. Lett. 41, 1055 (1978).

[49]See, e.g., A. Narath, A. T. Fromhold, Jr., and E. D. Jones, Phys. Rev. 144, 428 (1966).

[50]K. Terakura and J. Kanamori, Prog. Theor. Phys. 46, 1007 (1973).

[51]B. M. Klein and W. E. Pickett (unpublished).

[52]C. L. Wiley and F. Y. Fradin, Phys. Rev. B 17, 3462 (1978).

[53]R. P. Gupta and R. Benedek, Phys. Rev. B 22, 4572 (1979).